IEEE Access
Multidisciplinary | Rapid Review | Open Access Journal

Received January 29, 2019, accepted February 21, 2019, date of publication March 27, 2019, date of current version April 8, 2019.

Digital Object Identifier 10.1109/ACCESS.2019.2906868

Digital Manufacturing of Pathologically-Complex 3D Printed Antennas

KERRY JOHNSON[1], MICHAEL ZEMBA[2], BRETT P. CONNER[1], JASON WALKER[1], EDWARD BURDEN[1], KIRK ROGERS[3], KEVIN R. CWIOK[4], ERIC MACDONALD[1], AND PEDRO CORTES[1]

[1]Advanced Manufacturing Research Center, Youngstown State University, Youngstown, OH 44555, USA
[2]NASA Glenn Research Center, Cleveland, OH 44135, USA
[3]M&P Gravity Works LLC, North Lima, OH, USA
[4]Keselowski Advanced Manufacturing, Statesville, NC 28677, USA

Corresponding author: Kerry Johnson (kjohnson10@student.ysu.edu)

This work was supported in part by the National Science Foundation under Grant HRD 1432868, and in part by the Morris Friedman Endowment for Manufacturing at Youngstown State University, and Northern Ohio AGEP Alliance (NOA-AGEP).

ABSTRACT In the last decade, the proliferation of new 3D printing technologies has enabled the fabrication of complex geometries in manifold materials for novel applications. One discipline that has been explored extensively in the context of additive manufacturing is electromagnetic devices such as antennas. Difficult-to-fabricate geometries are now possible and can deliver new antenna functionality and extend performance (e.g., lower frequency resonance in small volumes, wider bandwidth, narrow-beam directionality, and so on). Coupled with accurate 3D electromagnetic simulations, a new paradigm is emerging for antenna design and manufacture. Starting from a seed geometry, the state space can now be explored to identify new combinations and permutations of electromagnetically-beneficial shapes through multiple simulation iterations. Subsequently, the identified structures can be further validated and improved through rapid manufacturing using 3D printing for hardware evaluation in an anechoic chamber. However, to fully benefit from this emerging paradigm, an up-to-date survey of the most recent metal processes is required. This survey would determine which processes are well suited for building the next generation of antennas. For this purpose, a variety of metal 3D printing was employed to fabricate benchmark antennas with pathological geometries, including thin walls, overhanging features, and large aspect ratios. This survey can inform designers about potential structures to serve in novel antennas. A total of five processes have been preliminarily explored including selective laser melting, binder jetting, and plated vat photopolymerization, all of which delivered different advantages and disadvantages in terms of mechanical and electromagnetic performance.

INDEX TERMS 3D printing, 3D printed antennas, 3D Hilbert curve, additive manufacturing, antenna radiation pattern, binder jetting, dipole antennas, fractal antenna, multifrequency antennas, powder-bed fusion, ultra high frequency, UHF, vat photopolymerization.

I. INTRODUCTION

Additive Manufacturing (AM), more popularly known as 3D printing, is impacting a wide range of industries with the ability to customize structures with complex geometries in high performance materials. One area that has received attention is in the fabrication of electromagnetic devices which stand to benefit from complex shapes. More recently, processes capable of printing metals and ceramics have made dramatic advances. Many of these emerging technologies have not yet been explored for application in the specific area of high-performance, next generation, freestanding antennas. This work seeks to identify newly available 3D printing processes that could be leveraged for electromagnetic devices and compare them in terms of electromagnetic, mechanical, thermal performance as well as manufacturability. The work cannot capture all emerging processes, but is a preliminary step to evaluate processes sufficiently mature to reliably fabricate pathologically-complex antennas. A benchmark antenna was identified that provided an agnostic example of

The associate editor coordinating the review of this manuscript and approving it for publication was Mingchun Tang.

a difficult-to-manufacture geometry - the Hilbert 3D fractal. The structure captures many of the challenging features that are not easily fabricated in traditional manufacturing, but are achievable with the latest additive manufacturing techniques. By simulating, fabricating, and evaluating a specific antenna, a new paradigm for exploring the antenna design space is demonstrated and recent manufacturing techniques are evaluated and compared in the contexts of fabricating antennas.

Substantial research has explored fabricating specific types of antennas. New AM processes allow for the embedding of electronic components into elaborate geometries in a stepwise manner that facilitates concurrent and sequential printing with collaborative manufacturing processes. Electrical connections have been realized with embedded conductive ink deposition for powering circuits and providing microprocessor communication [1]. Additionally, omnidirectional printing of conductive microstrips has been demonstrated for flexible circuits [2]. The utilization of conductive inks has been shown for generating traces on dielectric substrates for electromagnetic applications [3]–[12]. However, the conductivity of printed inks is restricted by the curing limits of the polymer; the metallic atoms dispersed within the binder-laden inks are inhibited from forming a high performance bulk conductor with only low temperature curing. One exception is with 3D printed ceramics as these dielectric structures can survive much higher temperatures and allow inks to eventually approach the performance of traditional plated copper. Embedding metallic wiring into 3D printed dielectrics has been evaluated as another solution to ink limitations [14], [15] resulting in electrical conductivity comparable to PCB traces.

The aim of this study is to identify which contemporary processes are well suited for creating complex and electrically conductive structures. In the field of 3D printing a taxonomy is used to categorize the processes based on the ISO/ASTM 52900 standard. 3D printing is a diverse landscape [16] with varying methods including the following seven subcategories:

- Powder Bed Fusion (metals and polymers),
- Material Extrusion (generally thermoplastics),
- Binder Jetting (generally metals or ceramics),
- Vat Photopolymerization (photocurable polymers),
- Material Jetting (metals, ceramics and photocurable polymers),
- Directed Energy Deposition (metals and ceramics)
- Sheet Lamination (paper, plastic, metal, composites).

Laser powder bed fusion (L-PBF) provides both polymers and metals. Selective laser sintering (subsumed in powder bed fusion) uses a laser to sinter a thermoplastic powder which is spread successively in thin layers. This process has been used to fabricate spherical wire antennas and waveguide antenna arrays [17], [18]. Selective Laser Melting is a similar process but focused on metals [19]. Peverini *et al.* [20] experimentally validated Ku/K-band filters for telecommunication developed using L-PBF . A waveguide array integrated into an antenna array was also successfully realized through the DMLS process [21]. The main drawbacks of L-PBF are poor surface finish, part density and residual stress. Zhang *et al.* [22] demonstrate the use of L-PBF in comparison with binder jetting for the development of antennas for millimeter and submillimeter wave applications.

Binder jetting likewise uses a powder bed, but with ink jetting to selectively eject a binder in order to consolidate powder. For metal printing, the resulting ''green parts'' are then sintered. With coarse powders, structures are infiltrated with a lower temperature melting metal to achieve a density close to 100%. For fine powders ($\sim$ 9 to 16 microns), nearly 100% density can be achieved with just sintering. This process provides ambient office-friendly conditions with a final high temperature furnace cycle. Binder jetting can potentially be used with any material that can be provided as a powder feedstock (sand, metal, polymer, ceramic, etc.). For the binder jetting of sand used in metal casting, there is no sintering step after printing as the curing of the foundry resin binder is sufficient to serve as disposable sand molds for metal casting.

Vat photopolymerization is a process in which a vat of material is selectively photopolymerized on a build plate that incrementally descends in the z-direction after each layer. Although, the resulting structures are not conductive, the smooth surface finish is well suited for subsequent plating of conductive metal layers. Both consumer and production printers are available for the process and can develop quality antenna components at relatively low costs [23]. Vat photopolymerization has proved fruitful for multiple waveguides designed to operate in the GHz frequency range [24], [25]. Chen *et al.* [26] advanced antennas further with the assembly of a novel 3D printed Fabry–Pérot Resonator antenna with paraboloid-shape superstrate for high gain, wide gain band applications. Horn antennas have also been fabricated through this process [27], yet, previous work on free-standing antennas with both complex geometries and expansive overhangs has not been published.

Material jetting provides the high spatial resolution of ink jetting and selectively deposits material (traditionally photocurable polymers but recently ceramics and metals as well) which is promptly UV and/or thermally cured. Many apparatuses utilizing this technology are capable of jetting separate materials simultaneously. A wide range of antennas that have been fabricated by the technology include: honeycomb and aperture-coupled antennas, patch antennas, Vivaldi, corrugated horn, phased array antenna, reflect array, waveguide slot antennas, and gradient index (GRIN) lens antennas [4], [7]–[10], [28]–[36]. Although polyjetting is one of the most pervasive material jetting techniques, the process is inherently restricted to UV curable photopolymers, which have reduced mechanical performance over time as the material continues to cure in the presence of UV light in the field.

The most ubiquitous AM method cited in the field of antennas is material extrusion additive manufacturing. In the last decade, many of the patents for this technology have expired and a bevy of open source and low cost desktop printers have been released - democratizing the field of 3D printing [37], [38]. Realization of thermoplastic fabricated

antennas has been enabled using various complementary means of metallization. One antenna was fabricated by a method of conductive infiltration of a substrate using Galinstan [39]. Bowtie, meandering line, and patch antennas have been created by using dual extrusion techniques to simultaneously deposit dielectric and conductive materials [11], [40], [41]. While a log-periodic array antenna was metalized by direct conductive ink printing [42], UAV embedded, fractal tree monopole, and triple mode horn antennas each have had surfaces selectively spray-coated with conductive ink [43]–[45]. Typical inconsistencies between measured and simulated results of conductive ink coated antennas suggest that electroplating or other bulk metal process are more suitable for antennas [32], [46] based on conductivity and surface finish.

While the aforementioned antenna geometries have various electromagnetic advantages, newly developed printers now allow for the fabrication of pathologically-complex free-standing, load-bearing metal antennas. Of these, fractal antennas may be an interesting application to use as a benchmark to compare each of these AM processes. The advantage of fractal antennas is for some or all of the following performance factors: multiband and broadband frequency behavior, sidelobe reduction, topological optimization, and beamforming algorithm capabilities [47], [48]. Many geometries have been tested to determine their potential antenna utility, notably: cross, hexagonal, concentric circular, tree, lighting, self-affining, and other unique fractal compositions, all of which have been evaluated in patch, slot, and/or 3D antenna studies [49]–[61]. However the most prominent fractal designs are versions of the Koch [62]–[68] and Sierpinski structures [69]–[74]. More recently, processes capable of printing metals and ceramics have made dramatic advances in spatial resolution and mechanical performance of the resulting structures, but many of the processes have not yet been explored for application in the specific area of high-performance, next generation antennas.

II. 3D SIMULATION AND FABRICATION METHODOLOGY

Advancements in electromagnetic simulation coupled with relentlessly-improving 3D printing processes are together enabling a new paradigm for exploring the design space of antennas. New geometries are available to be built in a wide variety of ceramics and polymers providing dielectrics with low loss and a wide range of permittivity. Moreover, metals can be printed serving as conductors with smooth surface finish and high conductivity. By optimizing antenna structures coarsely in simulation (virtual prototypes) and then fine-tuning the structure with many, rapid iterations of physical prototypes, an unprecedented study of a wide swathe of sculpted, next-generation antennas is now possible.

In this study, ANSYS HFSS was used to provide simulated frequency responses and 3D radiation patterns for the targeted geometries. These results were then later validated in hardware by fabricating the structure using five different additive manufacturing techniques and evaluating the electromagnetic performance in a far-field antenna range at NASA Glenn Research Center in Cleveland, Ohio. Other mechanical properties were also captured including total mass, density, surface finish and mechanical strength.

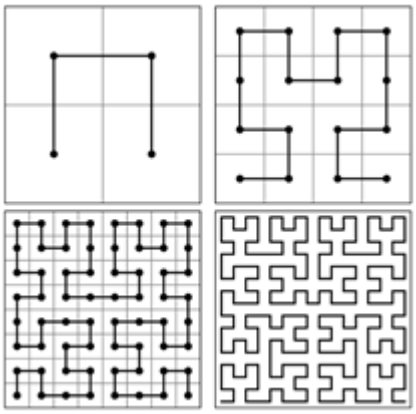

FIGURE 1. Increasing orders of 2D Hilbert Fractals.

A. BENCHMARK ANTENNA FOR PROCESS COMPARISION: 3D HILBERT FRACTAL

The 3D Hilbert Curve (HC) was selected for this study as the benchmark antenna as the antenna (1) has been studied in the past; (2) provides a challenging geometry to manufacture with 3D printing; and (3) maintains an agnostic application without proprietary implications. Previous work for the geometry through traditional manufacturing has been restricted to planar designs of patch, wire, and slot variations [75]–[78]. Recently, planar wire Hilbert curve antennas were deformed around a box to form a 3D design [79]. The HC can provide small resonant antennas that efficiently fill space with a continuous conductive line. Given that infinite resolution is not realizable for manufactured devices, these designs can be referred to as pre-fractals meaning that the design is fabricated to approach full self-similarity and resolution by increasing the order of iterations used to fractalize the geometry (Fig. 1). The resonant nature of the antenna changes as the order increases, with wire diameter being an important property, affecting the space-filling efficiency and Q-factor.

For this manufacturing survey, the Hilbert was fully extended to 3D (Fig. 2), as this structure requires high aspect ratio struts in all six orthogonal directions (parallel to the X, Y, Z, -X, -Y, and -Z directions). For additive manufacturing specifically, this geometry is challenging as there are many overhanging features and each side of the Hilbert dipole includes a circuitous length (over 115 cm when fully extended in a straight line). Compounded by the length, the 3D serpentine nature lead to intentional destabilization, which is necessary to comprehensively evaluate the mechanical properties. The full antenna includes 63 1.96 cm segments (a total length of 1.23 m) that sweep in one of six 90 degree turns to

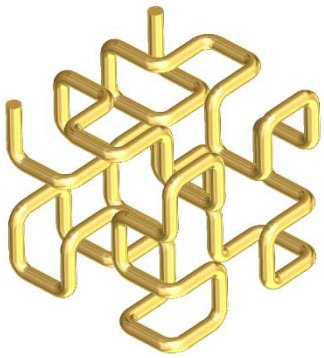

FIGURE 2. Baseline structure - the 3D Hilbert Fractal (isometric view).

begin each new segment. The struts were 3.7 mm in diameter including at the swept turns.

For the purposes of this study, there was no specific application for the antenna (targeted communication link, resonant frequency or directionality). The authors were resolute in maintaining an agnostic and generic application that could serve well as a general comparison of 3D electromagnetic simulations against several 3D printing techniques. The compact nature of the fractal geometry results in an antenna that resonates at low frequencies relative to the overall occupied volume and fits inside of a 1U CubeSat format (10 cm cubed) which provides potential utility for university space science. The geometrical characteristics therefore provide a sound benchmark for extrapolating to other antenna geometries with simulation and 3D printing in order to demonstrate the new antenna design paradigm.

B. ELECTROMAGNETIC SIMULATION

Several high-fidelity software packages are available to provide 3D electromagnetic simulations for curved geometries, and in this study, ANSYS HFSS was selected. The Hilbert geometry in Fig. 2 was simulated using perfect electrically conducting material and both the frequency response as well as the radiation pattern at the peak resonant frequency were captured (Fig. 3 & 4). Simulation results suggests that the antenna has an omnidirectional radiation pattern at a central, narrowband frequency of approximately 1.4 GHz. Wideband behavior was recognized between -5 and -10 dB, from roughly 1.5-2 GHz - future investigations could further optimize this behavior.

III. ADDITIVE MANUFACTURING (3D PRINTING) PROCESS SURVEY

The market introduction of several new metals 3D printing processes inspired this survey but at the time of this experiment, these processes were not sufficiently mature or available to be included in the final experiment. Both Desktop Metal (Boston USA) and Markforged (Boston USA) declined to fabricate the geometry and are currently developing relatively low-cost metal processes which can potentially create the Hilbert antenna geometry in copper. With bulk-like performance at least to a depth of 5-8 mm from the superficial surfaces depending on debinding, these processes can add new materials and more geometries to the discussion. However, other more mature 3D printing technologies were available and used but not directly with copper.

Copper provides high conductivity (σ at 20 °C $\approx 5.96 \times 10^7$ [S/m]) and reasonable strength and rigidity. Aluminum alloys, alternatively, provide about 30 to 60% the conductivity of copper but with reduced weight. Steel infiltrated with bronze was also explored in this case which delivered roughly 20% of the conductivity of copper but with much higher mechanical performance and with the expense of increased weight. Finally, the use of non-conductive polymer structural material was explored and then the structure was

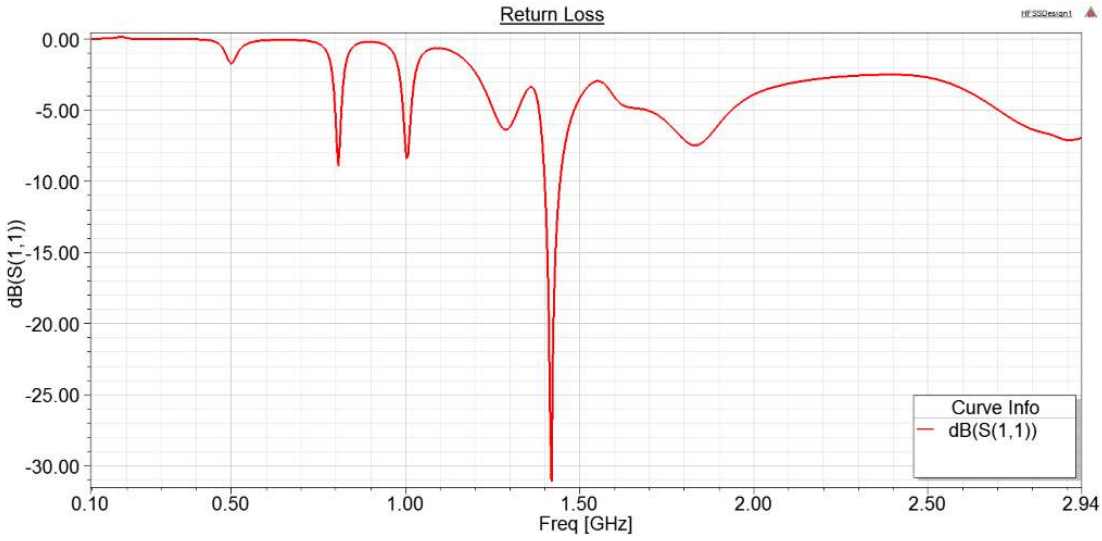

FIGURE 3. Return loss (S11 in dB) vs. frequency (GHz) for the 3D Hilbert antenna as simulated in Ansys HFSS.

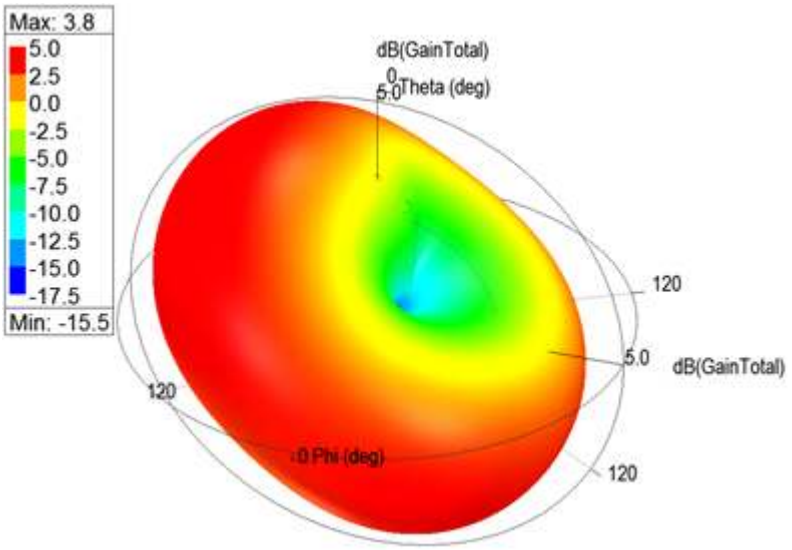

FIGURE 4. Radiation pattern at the resonant frequency of 1.41 GHz and isometric orientation as simulated in Ansys HFSS.

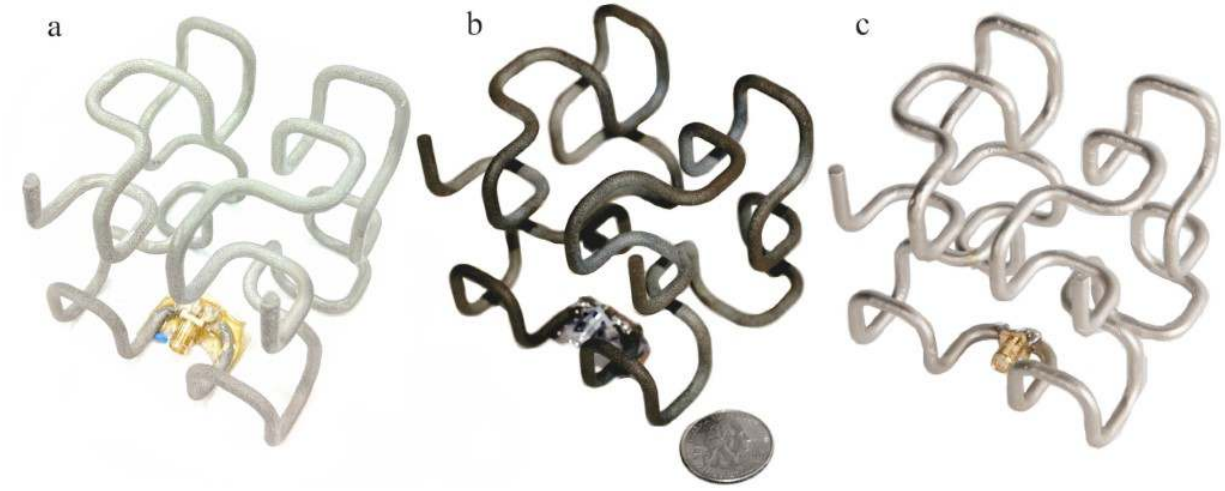

FIGURE 5. (a) EOS M280 (L-PBF), (b) ExOne M-FLEX (binder jetting), (c) Formlabs (Vat Photopolymerization with plating) with a quarter for reference.

later plated with copper and nickel to provide the necessary conductivity and this option allowed for much lighter structures but with substantially reduced strength. Each of these material options described above could be beneficial to a wide variety of antennas depending on the application and conditions (e.g. subjected to loads such as accelerations or aerodynamic drag).

A. LIST OF TARGETED 3D PRINTING PROCESSES

Table 1 lists the five cases that were fabricated. In addition, the first three processes were evaluated at NASA Glenn Research Center (GRC). The fourth was evaluated only in terms of the frequency response using a Vector Network Analyzer as this antenna was manufactured 4.5 times larger due to minimum features size constraints of the specific 3D printing process. For this larger antenna, the radiation pattern is expected to be similar to the smaller geometry in terms of directivity but translated to a lower frequency as a function of the geometry scaling factor.

Of the five AM processes used to fabricate the Hilbert antenna, three sufficiently met the intended dimensional criteria and were evaluated at NASA Glenn Research Center by both VNA and far-field radiation pattern measurement. 3DMT, LLC (Daytona Beach, USA) provided the fabrication with an EOS M280 system, printing AlSi10Mg using a form of powder bed fusion referred to as selective laser melting. ExOne, Inc. (North Huntingdon, USA) provided fabrication services for a fee with the company's M-FLEX binder jetting system. This system bound 316L steel powder which was

TABLE 1. The antenna fabrication specifications.

Process	System	Material	Comment
Laser powder-bed fusion	EOS M290	AlSi10Mg	Evaluated at GRC
Binder jetting	ExOne M-FLEX	316L Steel with Bronze infiltration	Evaluated at GRC
Vat Photopolymerization	Formlabs Form II	Copper/Nickel-plated	Evaluated at GRC
Binder jetting, polymerization, plating	Freshmade 3D	Copper/Chrome-plated	VNA evaluated
Binder jetting of sand mold and casting	ExOne S-MAX	Al 356	N/A

FIGURE 6. Polymerized bound sand with plating.

later sintered and infiltrated with bronze to provide close to full density in a multi-metal matrix. The third antenna was manufactured with the Formlabs Form 2 Stereolithography 3D printer in a clear resin. After an Isopropyl alcohol bath and UV cure, the SLA print was subsequently electroplated with copper/tin by RePliForm, Inc., (Baltimore, USA). Fig. 5 shows the three resulting structures of these processes.

Additionally, a proprietary engineered particulate composite (EPC), which was enabled by binder jetting process [80] was used by Freshmade3D, LLC (Youngstown, OH) in which binder jetted sand structures were create using the ExOne S-MAX, functionalized and then copper and chrome plated (Fig 6.). However, the minimum feature sizes of the target Hilbert were not possible so an antenna 4.5 times larger was produced. The resulting antenna was not evaluated at NASA as the resonant frequencies were too low for the far-field range but the S11 response was measured with a vector network analyzer at Youngstown State University and the antenna provided expected performance but with frequency scaled inversely proportional to the volume. Finally, a 3D printed sand mold was printed using the ExOne S-MAX printer at Youngstown State University and one half of the

TABLE 2. Process geometric accuracy.

	CAD	EOS M290	ExOne M-FLEX	Form II
Strut Diameter	3.70	3.82	3.75	3.82
% Error		3.24	1.35	3.24
Full Side Length	68.7	68.59	69.21	69.01
% Error		0.16	0.74	0.45
Height	68.7	68.47	69.07	68.47
% Error		0.33	0.54	0.33
Mass (g)		34	105	28
Density (g/cm^3)		3.2	10.0	2.7
Discrete RMS Surface Roughness (μm)		9.20	6.79	5.34
Mechanical Strength		Good	Great	Poor

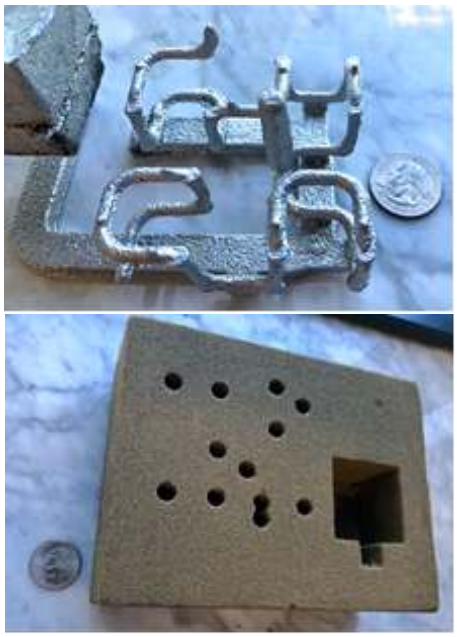

FIGURE 7. Cast aluminum with a 3D printed sand mold.

dipole antenna was cast with aluminum A356, however the dimensional accuracies and surface finish were not sufficient to pursue this antenna further at these small dimensions. The final cast structure including gating and sprue are shown in Fig. 7.

IV. RESULTS AND DISCUSSION

The 3D printed antennas that met design criteria were evaluated both mechanically (e.g. surface roughness, strength,

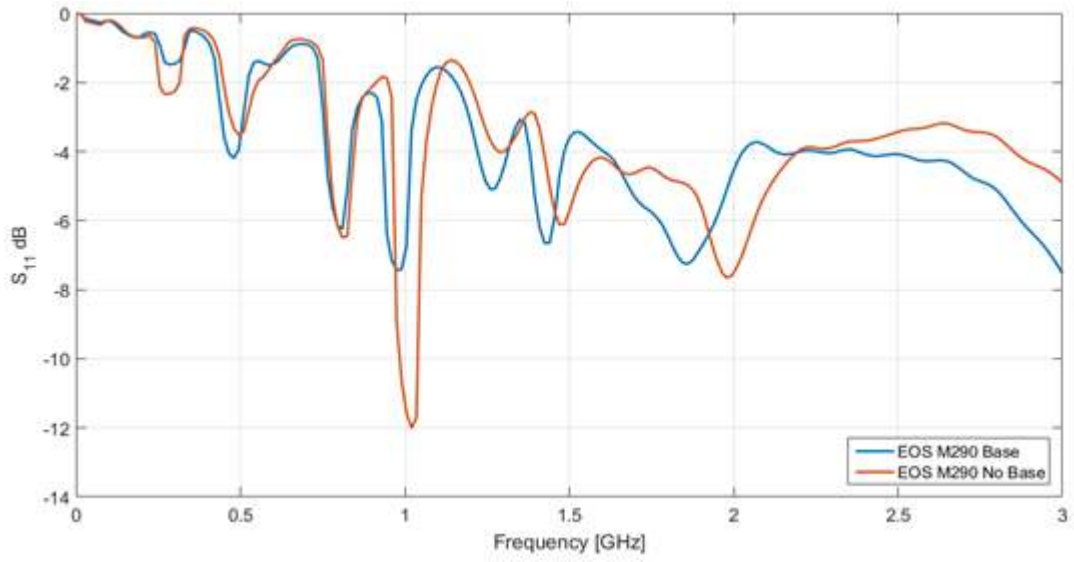

FIGURE 8. VNA results of SLM with and without the dielectric base.

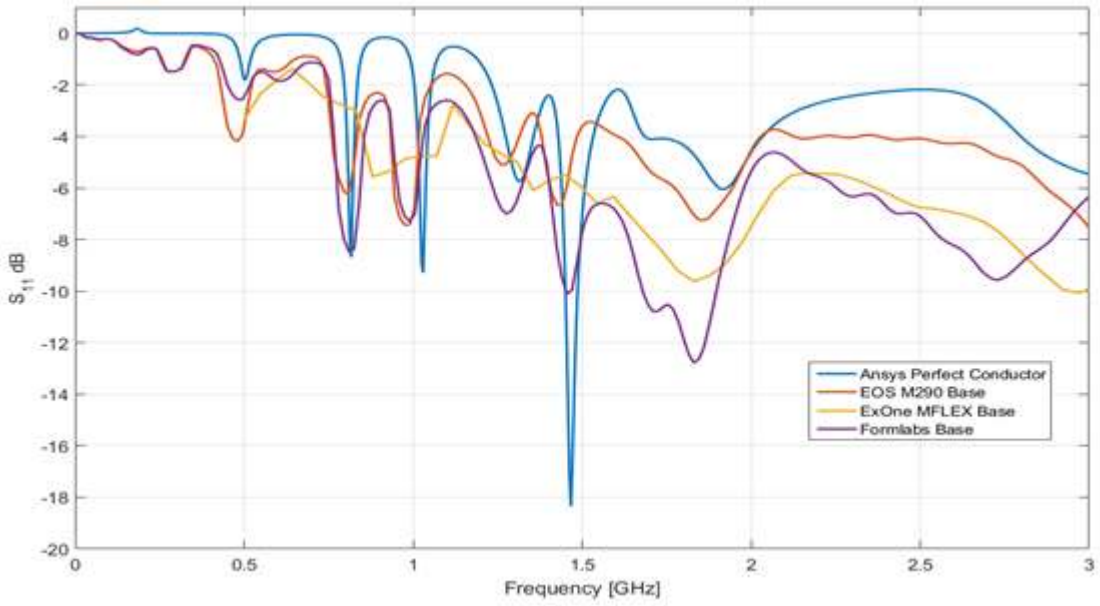

FIGURE 9. VNA comparison between processes and simulation.

weight, etc.) as well as electrically (e.g. conductivity, electromagnetic performance, etc.).

A. MECHANICAL PERFORMANCE

Table 2 shows for each case the dimensional error, mass, density, surface finish grading, mass, and reported strength. Also included are comments about relative expense and post processing required to finish the antennas. Depending on the application requirements for a specific antenna, all of these characteristics could be prioritized or weighted differently and consequently any one of these processes could be the most suitable for a given application depending on frequency, directionality and mechanical properties.

Initially, each side of the dipole was attached to an SMA connector with a combination of solder and Abelbond 84-1LMI silver conductive adhesive. Subsequently, for added stability purposes, a simple two-part epoxy is coated around the connection point. Connection imperfections, in conjunction with geometric deformations due to residual stresses caused some static canting and wobbling in the antenna which affected the performance of the antennas by modifying the geometries slightly.

Profilometry, using the Alpha-Step D-100 profilometer, was done to determine the discrete rms surface finish of each part. However, at the relatively low frequencies being studied, the surface roughness was not an impediment.

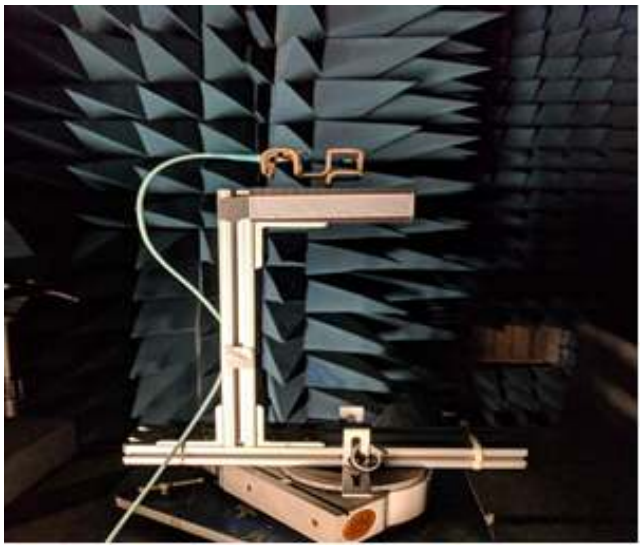

FIGURE 10. Radiation pattern measurement in the far-field antenna range at NASA Glenn Research Center.

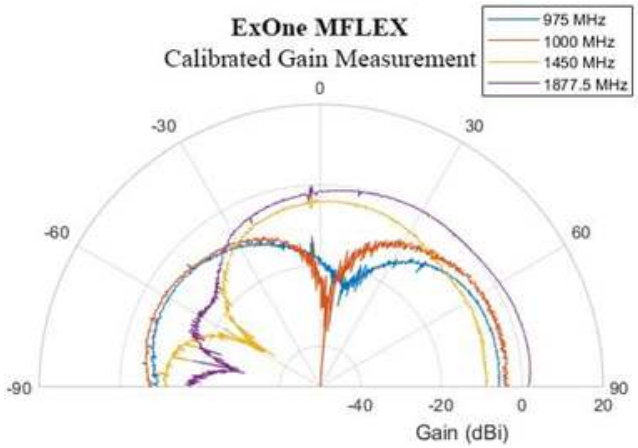

FIGURE 11. ExOne MFLEX calibrated radiation pattern at pertinent frequencies.

Below 10 GHz for instance, the wavelength is 30 mm or more and the surface roughness of most AM processes is several orders of magnitude smaller. The EOS M280 system produced the highest roughness, followed by the ExOne M-FLEX part. The Form II antenna had the lowest and most quasi-periodic surface finish. The mechanical properties of the antennas varied widely. The L-PBF and binder jetted antennas were rigid, with the SLA component having flexible and lightweight characteristics and may be suitable for applications with weight restrictions.

B. ELECTROMAGNETIC PERFORMANCE

The antennas were tested at NASA Glenn Research Center using a VNA and far-field antenna range. The VNA measurements were taken for each antenna with and without a polymer ABS base container of 0.5 cm thickness, which was used to provide additional mechanical support by providing a cavity for the bounding box of the Hilbert at the bottom 17% of the structure, at any orientation. The negative peaks in the plot of the reflection coefficient (see Fig. 8) correspond to frequencies where the antenna showed the best transmission of signal. There was an observed frequency shift of the resonance peaks and an increase in the magnitude of transmitted signal when the base was removed. This could be the result of a change in the input impedance of the antenna as well as canting of the mechanical connection of the SMA jack to the antenna. The SLA part provided the greatest combined gain and multiband behavior, while the binder jetted antenna had decent gain, but displayed relatively poor multiband characteristics. The best all-around performance came from the L-PBF aluminum exhibiting median gain and decent multiband performance (see Fig. 9).

The radiation patterns for all three of the antennas under test (AUT) were initially obtained in the far-field anechoic chamber at NASA Glenn with the setup displayed below

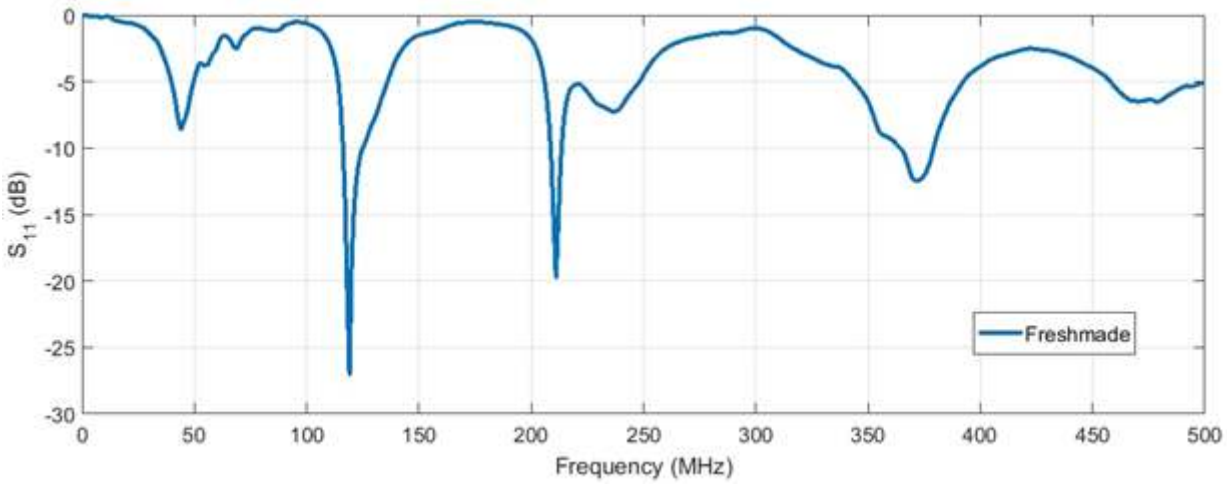

FIGURE 12. VNA measurement of Freshmade3D antenna.

(see Fig 10). However, revaluation was done for normalization using the binder jetted part and a reference antenna of known gain (Fig. 11). The antenna azimuth was swept in quarter degree increments from 0° to 180° with constant elevation angle. The radiation pattern was characterized at 0.975, 1, 1.41, and 1.8775 GHz based on the resonant frequencies observed during VNA testing. The AUT showed decent performance relative to an isotropic radiator.

Additionally, VNA testing was conducted on the larger scale Freshmade3D antenna (Fig. 12). Though the antenna resonated at much lower frequencies as expected, the S_{11} results exhibited similar characteristics as translated to the lower frequencies. However, stronger resonance (−27 dB) occurred for this antenna at the target frequencies.

The resulting S11 measurements and radiation patterns were overall in reasonable agreement with the simulation output. However, differences were measured between the antennas and simulations. Aside from obvious issues of canting and wobbling that occurred, electromagnetic issues manifested from a materials standpoint. Phenomena such as the skin effect which was impacted by the imperfect surface finish resulted in target resonance frequencies discrepancies. This deviations from the nominal geometries explain why the Formlabs model performed better at higher frequencies than the binder jetted or SLA counterparts which are generally considered rougher.

V. CONCLUSIONS

This study demonstrated a new paradigm in the design and manufacture of antennas which leverages both high fidelity electromagnetic simulation tools (to create virtual prototypes) coupled with a range of contemporary additive manufacturing processes (to create physical prototypes). By simulating and fabricating a pathologically-complex Hilbert Fractal antenna in several 3D printing processes and evaluating these in an anechoic chamber, simulations were validated through several rapidly-manufactured physical examples. The successful antennas were created with a high degree of accuracy across an array of manufacturing processes including:

- Powder Bed Fusion: An EOS M280 printed the structure in AlSi10Mg which was relatively light, strong, relatively conductive (with 25.69% of the conductivity of copper), accurate, and sufficiently smooth with a surface finish reasonable for frequencies under 30 GHz.
- Binder Jetting of Metal: An ExOne M-FLEX printed the structure in 316L steel and bronze which was relatively heavy, strong, conductive (with 7.78% of the conductivity of copper), accurate, and sufficiently smooth with a surface finish reasonable for frequencies under 30 GHz.
- Vat Photopolymerization with Plating: A FormLabs 2 printed the structure in a photocurable polymer and then plated with copper and tin which was very light, conductive (with 70.96% of the conductivity of copper), accurate, and very smooth with a surface finish reasonable for frequencies extending beyond 30 GHz.

Future work will include extending the study to material extrusion of Metal Injection Molding (MIM) feedstocks from companies like Desktop Metal and MarkForged as well as standard printers using new MIM materials available from BASF. Other processes which may hold promise for the fabrication of larger antennas include polymerized binder jetted sand from Freshmade3D LLC as well as sand casting with 3D printed molds. Antennas fabricated with either process were not possible in the small dimensions targeted by this study; however, for low frequency applications, these processes may be better suited than the rest. New ceramic processes offer the ability to create a low loss substrate that can sustain the high temperatures required to fully cure and melt nanoparticle metal inks and this combination of dielectric and conductor could enable new applications as well.

ACKNOWLEDGMENT

The authors would like to respectfully acknowledge NASA Glenn Research Center for the use of their facilities for antenna evaluation, and 3DMT, ExOne, and Freshmade3D for supporting this research by fabricating antennas in manifold processes. Any opinions, findings, and conclusions or recommendations expressed in this material are those of the author(s) and do not necessarily reflect the views of the National Science Foundation.

REFERENCES

[1] E. MacDonald *et al.*, "3D printing for the rapid prototyping of structural electronics," *IEEE Access*, vol. 2, pp. 234–242, 2014.
[2] B. Y. Ahn *et al.*, "Omnidirectional printing of flexible, stretchable, and spanning silver microelectrodes," *Science*, vol. 323, no. 5921, pp. 1590–1593, 2009.
[3] J. J. Adams *et al.*, "Conformal printing of electrically small antennas on three-dimensional surfaces," *Adv. Mater.*, vol. 23, no. 11, pp. 1335–1340, Mar. 2011.
[4] J. A. Paulsen, M. Renn, K. Christenson, and R. Plourde, "Printing conformal electronics on 3D structures with aerosol jet technology," in *Proc. Future Instrum. Int. Workshop (FIIW)*, Oct. 2012, pp. 1–4.
[5] B. Y. Ahn *et al.*, "Planar and three-dimensional printing of conductive inks," *J. Vis. Exp.*, vol. 58, p. e3189, Dec. 2011. doi: 10.3791/3189.
[6] P. J. Smith, D.-Y. Shin, J. E. Stringer, B. Derby, and N. Reis, "Direct ink-jet printing and low temperature conversion of conductive silver patterns," *J. Mater. Sci.*, vol. 41, no. 13, pp. 4153–4158, Jul. 2006.
[7] T. P. Ketterl, "A 2.45 GHz phased array antenna unit cell fabricated using 3-D multi-layer direct digital manufacturing," *IEEE Trans. Microw. Theory Techn.*, vol. 63, no. 12, pp. 4382–4394, Dec. 2015.
[8] I. T. Nassar, T. M. Weller, and H. Tsang, "3-D printed antenna arrays for harmonic radar applications," in *Proc. Wireless Microw. Technol. Conf. (WAMICON)*, Jun. 2014, pp. 1–4.
[9] M. Mirzaee, "Developing novel 3D antennas using advanced additive manufacturing technology," Univ. North Dakota, Grand Forks, ND, USA, Tech. Rep., 2015. [Online]. Available: http://adsabs.harvard.edu/abs/2015PhDT.....210M
[10] N. Arnal *et al.*, "3D multi-layer additive manufacturing of a 2.45 GHz RF front end," in *IEEE MTT-S Int. Microw. Symp. Dig.*, May 2015, pp. 1–4.
[11] M. Liang, C. Shemelya, E. MacDonald, R. Wicker, and H. Xin, "Fabrication of microwave patch antenna using additive manufacturing technique," in *Proc. USNC-URSI Radio Sci. Meeting (Joint With AP-S Symp.)*, Jul. 2014, p. 269.
[12] C. Shemelya *et al.*, "3D printed capacitive sensors," in *Proc. IEEE Sensors*, Nov. 2013, pp. 1–4.
[13] J. M. O'Brien, J. E. Grandfield, G. Mumcu, and T. M. Weller, "Miniaturization of a spiral antenna using periodic Z-plane meandering," *IEEE Trans. Antennas Propag.*, vol. 63, no. 4, pp. 1843–1848, Apr. 2015.

[14] E. MacDonald and R. Wicker, "Multiprocess 3D printing for increasing component functionality," *Science*, vol. 353, no. 6307, Sep. 2016, Art. no. aaf2093.
[15] D. Espalin, D. W. Muse, E. MacDonald, and R. B. Wicker, "3D printing multifunctionality: Structures with electronics," *Int. J. Adv. Manuf. Technol.*, vol. 72, nos. 5–8, pp. 963–978, 2014.
[16] M. Liang and H. Xin, "Three-dimensionally printed/additive manufactured antennas," in *Handbook of Antenna Technologies*, Z. N. Chen, D. Liu, H. Nakano, X. Qing, and T. Zwick, Eds. Singapore: Springer, 2016, pp. 661–697.
[17] G.-L. Huang, S.-G. Zhou, T.-H. Chio, and T.-S. Yeo, "Fabrication of a high-efficiency waveguide antenna array via direct metal laser sintering," *IEEE Antennas Wireless Propag. Lett.*, vol. 15, pp. 622–625, 2016.
[18] O. S. Kim, "Rapid prototyping of electrically small spherical wire antennas," *IEEE Trans. Antennas Propag.*, vol. 62, no. 7, pp. 3839–3842, Jul. 2014.
[19] *EOS Electro Optical Systems: Industrial 3D Printing*. Accessed: Jun. 25, 2018. [Online]. Available: https://www.eos.info/en
[20] O. A. Peverini *et al.*, "Selective laser melting manufacturing of microwave waveguide devices," *Proc. IEEE*, vol. 105, no. 4, pp. 620–631, Apr. 2017.
[21] H. Guan-Long, Z. Shi-Gang, C. Tan-Huat, and Y. Tat-Soon, "3-D metal-direct-printed wideband and high-efficiency waveguide-fed antenna array," in *IEEE MTT-S Int. Microw. Symp. Dig.*, May 2015, pp. 1–4.
[22] B. Zhang *et al.*, "Metallic 3-D printed antennas for millimeter- and submillimeter wave applications," *IEEE Trans. THz Sci. Technol.*, vol. 6, no. 4, pp. 592–600, Jul. 2016.
[23] B. Rohrdantz, C. Rave, and A. F. Jacob, "3D-printed low-cost, low-loss microwave components up to 40 GHz," in *IEEE MTT-S Int. Microw. Symp. Dig.*, May 2016, pp. 1–3.
[24] E. G. Geterud, P. Bergmark, and J. Yang, "Lightweight waveguide and antenna components using plating on plastics," in *Proc. 7th Eur. Conf. Antennas Propag. (EuCAP)*, Apr. 2013, pp. 1812–1815.
[25] G. P. Le Sage, "3D printed waveguide slot array antennas," *IEEE Access*, vol. 4, pp. 1258–1265, 2016.
[26] Q. Chen, X. Chen, and K. Xu, "3-D printed fabry–pérot resonator antenna with paraboloid-shape superstrate for wide gain bandwidth," *Appl. Sci.*, vol. 7, no. 11, p. 1134, Nov. 2017.
[27] Y. Huang, X. Gong, S. Hajela, and W. J. Chappell, "Layer-by-layer stereolithography of three-dimensional antennas," in *Proc. IEEE Antennas Propag. Soc. Int. Symp.*, vol. 1A, Jul. 2005, pp. 276–279.
[28] G. McKerricher, D. Titterington, and A. Shamim, "A fully inkjet-printed 3-D honeycomb-inspired patch antenna," *IEEE Antennas Wireless Propag. Lett.*, vol. 15, pp. 544–547, 2016.
[29] K. A. Nate, J. Hester, M. Isakov, R. Bahr, and M. M. Tentzeris, "A fully printed multilayer aperture-coupled patch antenna using hybrid 3D / inkjet additive manufacturing technique," in *Proc. Eur. Microw. Conf. (EuMC)*, Sep. 2015, pp. 610–613.
[30] M. I. M. Ghazali, K. Y. Park, J. A. Byford, J. Papapolymerou, and P. Chahal, "3D printed metalized-polymer UWB high-gain Vivaldi antennas," in *IEEE MTT-S Int. Microw. Symp. Dig.*, May 2016, pp. 1–4.
[31] E. Decrossas, T. Reck, C. Lee, C. Jung-Kubiak, I. Mehdi, and G. Chattopadhyay, "Evaluation of 3D printing technology for corrugated horn antenna manufacturing," in *Proc. IEEE Int. Symp. Electromagn. Compat. (EMC)*, Jul. 2016, pp. 251–255.
[32] B.-J. Chen, H. Yi, K. B. Ng, S.-W. Qu, and C. H. Chan, "3D printed reflectarray antenna at 60 GHz," in *Proc. Int. Symp. Antennas Propag. (ISAP)*, Oct. 2016, pp. 92–93.
[33] G. McKerricher, A. Nafe, and A. Shamim, "Lightweight 3D printed microwave waveguides and waveguide slot antenna," in *Proc. IEEE Int. Symp. Antennas Propag. USNC/URSI Nat. Radio Sci. Meeting*, Jul. 2015, pp. 1322–1323.
[34] C. M. Shemelya, M. Zemba, C. Kief, D. Espalin, R. B. Wicker, and E. MacDonald, "Multi-layer off-axis patch antennas fabricated using polymer extrusion 3D printing," in *Proc. 10th Eur. Conf. Antennas Propag. (EuCAP)*, Apr. 2016, pp. 1–5.
[35] P. Nayeri *et al.*, "3D printed dielectric reflectarrays: Low-cost high-gain antennas at sub-millimeter waves," *IEEE Trans. Antennas Propag.*, vol. 62, no. 4, pp. 2000–2008, Apr. 2014.
[36] M. Liang, W. R. Ng, K. Chang, K. Gbele, M. E. Gehm, and H. Xin, "A3-D Luneburg lens antenna fabricated by polymer jetting rapid prototyping," *IEEE Trans. Antennas Propag.*, vol. 62, no. 4, pp. 1799–1807, Apr. 2014.
[37] I. Gibson, D. Rosen, and B. Stucker, *Additive Manufacturing Technologies: 3D Printing, Rapid Prototyping, and Direct Digital Manufacturing*. New York, NY, USA: Springer-Verlag, 2014. [Online]. Available: https://www.springer.com/gp/book/9781493921126
[38] C. Rodriguez, J. Avila, and R. C. Rumpf, "Ultra-thin 3D printed all-dielectric antenna," *Prog. Electromagn. Res. C*, vol. 64, pp. 117–123, May 2016.
[39] M. Cosker, F. Ferrero, L. Lizzi, R. Staraj, and J.-M. Ribero, "3D flexible antenna realization process using liquid metal and additive technology," in *Proc. IEEE Int. Symp. Antennas Propag. (APSURSI)*, Jun./Jul. 2016, pp. 809–810.
[40] M. Mirzaee, S. Noghanian, L. Wiest, and I. Chang, "Developing flexible 3D printed antenna using conductive ABS materials," in *Proc. IEEE Int. Symp. Antennas Propag. USNC/URSI Nat. Radio Sci. Meeting*, Jul. 2015, pp. 1308–1309.
[41] M. Ahmadloo and P. Mousavi, "A novel integrated dielectric-and-conductive ink 3D printing technique for fabrication of microwave devices," in *IEEE MTT-S Int. Microw. Symp. Dig.*, Jun. 2013, pp. 1–3.
[42] I. T. Nassar, T. M. Weller, and H. Tsang, "A 3-D printed miniaturized log-periodic dipole antenna," in *Proc. IEEE Antennas Propag. Soc. Int. Symp. (APSURSI)*, Jul. 2014, pp. 11–12.
[43] K. V. Hoel, S. Kristoffersen, J. Moen, G. Holm, and T. S. Lande, "Characterization of a 3D printed wideband waveguide and horn antenna structure embedded in a UAV wing," in *Proc. 10th Eur. Conf. Antennas Propag. (EuCAP)*, Apr. 2016, pp. 1–4.
[44] A. T. Castro and S. K. Sharma, "A triple mode waveguide corrugated horn antenna using 3D printing technology," in *Proc. IEEE Int. Symp. Antennas Propag. USNC/URSI Nat. Radio Sci. Meeting*, Jul. 2017, pp. 1235–1236.
[45] K. Smith and R. Adams, "A broadband 3D printed fractal tree monopole antenna," *Prog. Electromagn. Res. C*, vol. 86, pp. 17–28, Jul. 2018.
[46] Y. Tawk, M. Chahoud, M. Fadous, J. Costantine, and C. G. Christodoulou, "The miniaturization of a partially 3-D printed quadrifilar helix antenna," *IEEE Trans. Antennas Propag.*, vol. 65, no. 10, pp. 5043–5051, Oct. 2017.
[47] D. H. Werner and S. Ganguly, "An overview of fractal antenna engineering research," *IEEE Antennas Propag. Mag.*, vol. 45, no. 1, pp. 38–57, Feb. 2003.
[48] D. H. Werner, R. L. Haupt, and P. L. Werner, "Fractal antenna engineering: The theory and design of fractal antenna arrays," *IEEE Antennas Propag. Mag.*, vol. 41, no. 5, pp. 37–58, Oct. 1999.
[49] S. Y. Jun, B. Sanz-Izquierdo, E. A. Parker, D. Bird, and A. McClelland, "Manufacturing considerations in the 3-D printing of fractal antennas," *IEEE Trans. Compon. Packag. Manuf. Technol.*, vol. 7, no. 11, pp. 1891–1898, Nov. 2017.
[50] J. Chang and S. Lee, "Hybrid fractal cross antenna," *Microw. Opt. Technol. Lett.*, vol. 25, no. 6, pp. 429–435, Jun. 2000.
[51] A. Azari, "A new super wideband fractal microstrip antenna," *IEEE Trans. Antennas Propag.*, vol. 59, no. 5, pp. 1724–1727, May 2011.
[52] P. W. Tang and P. F. Wahid, "Hexagonal fractal multiband antenna," *IEEE Antennas Wireless Propag. Lett.*, vol. 3, pp. 111–112, 2004.
[53] J. Pourahmadazar, C. Ghobadi, J. Nourinia, and H. Shirzad, "Multiband ring fractal monopole antenna for mobile devices," *IEEE Antennas Wirel. Propag. Lett.*, vol. 9, pp. 863–866, 2010.
[54] C. Varadhan, J. K. Pakkathillam, M. Kanagasabai, R. Sivasamy, R. Natarajan, and S. K. Palaniswamy, "Triband antenna structures for RFID systems deploying fractal geometry," *IEEE Antennas Wireless Propag. Lett.*, vol. 12, pp. 437–440, 2013.
[55] J. A. Valdivia, G. Milikh, and K. Papadopoulos, "Red sprites: Lightning as a fractal antenna," *Geophys. Res. Lett.*, vol. 24, no. 24, pp. 3169–3172, Dec. 1997.
[56] M. Ding, R. Jin, J. Geng, and Q. Wu, "Design of a CPW-fed ultrawideband fractal antenna," *Microw. Opt. Technol. Lett.*, vol. 49, no. 1, pp. 173–176, Jan. 2007.
[57] A. G. Lopez, E. E. Lopez C., R. Chandra, and A. J. Johansson, "Optimization and fabrication by 3D printing of a volcano smoke antenna for UWB applications," in *Proc. 7th Eur. Conf. Antennas Propag. (EuCAP)*, Apr. 2013, pp. 1471–1473.
[58] S. N. Sinha and M. Jain, "A self-affine fractal multiband antenna," *IEEE Antennas Wireless Propag. Lett.*, vol. 6, pp. 110–112, 2007.
[59] O. M. Khan, R. M. Shubair, and Q. U. Islam, "Second order flamenco fractal antenna for industrial scientific and medical applications," in *Proc. Int. Conf. Elect. Comput. Technol. Appl. (ICECTA)*, Nov. 2017, pp. 1–3.
[60] V. V. Reddy, "Single-feed circularly polarized flared-U fractal boundary microstrip antenna," *IETE J. Res.*, vol. 63, no. 4, pp. 577–587, Mar. 2017.
[61] V. Sharma, N. Lakwar, N. Kumar, and T. Garg, "Multiband low-cost fractal antenna based on parasitic split ring resonators," *IET Microw., Antennas Propag.*, vol. 12, no. 6, pp. 913–919, May 2017.
[62] F. Viani, M. Salucci, F. Robol, G. Oliveri, and A. Massa, "Design of a UHF RFID/GPS fractal antenna for logistics management," *J. Electromagn. Waves Appl.*, vol. 26, no. 4, pp. 480–492, Jan. 2012.

[63] C. P. Baliarda, J. Romeu, and A. Cardama, "The Koch monopole: A small fractal antenna," *IEEE Trans. Antennas Propag.*, vol. 48, no. 11, pp. 1773–1781, Nov. 2000.
[64] D. Li and J.-F. Mao, "A koch-like sided fractal bow-tie dipole antenna," *IEEE Trans. Antennas Propag.*, vol. 60, no. 5, pp. 2242–2251, May 2012.
[65] X. Liang and M. Y. W. Chia, "Multiband characteristics of two fractal antennas," *Microw. Opt. Technol. Lett.*, vol. 23, no. 4, pp. 242–245, Nov. 1999.
[66] E. Lule and T. Babij, "Koch island fractal ultra wideband dipole antenna," in *Proc. IEEE Antennas Propag. Soc. Symp.*, vol. 3, Jun. 2004, pp. 2516–2519.
[67] S. K. Terlapu, J. Cheruku, and G. Raju, "On the notch band characteristics of koch fractal antenna for UWB applications," *Int. J. Control Theory Appl.*, vol. 10, no. 6, pp. 701–707, Apr. 2017.
[68] E. P. Bellido, G. D. Bernasconi, D. Rossouw, J. Butet, O. J. F. Martin, and G. A. Botton, "Self-similarity of plasmon edge modes on koch fractal antennas," *ACS Nano*, vol. 11, no. 11, pp. 11240–11249, Nov. 2017.
[69] R. A. Bahr, Y. Fang, W. Su, B. Tehrani, V. Palazzi, and M. M. Tentzeris, "Novel uniquely 3D printed intricate Voronoi and fractal 3D antennas," in *IEEE MTT-S Int. Microw. Symp. Dig.*, Jun. 2017, pp. 1583–1586.
[70] C. Puente, J. Romeu, R. Pous, X. Garcia, and F. Benitez, "Fractal multiband antenna based on the Sierpinski gasket," *Electron. Lett.*, vol. 32, no. 1, pp. 1–2, Jan. 1996.
[71] C. Puente-Baliarda, J. Romeu, R. Pous, and A. Cardama, "On the behavior of the Sierpinski multiband fractal antenna," *IEEE Trans. Antennas Propag.*, vol. 46, no. 4, pp. 517–524, Apr. 1998.
[72] D. Shamvedi, O. J. McCarthy, E. O'Donoghue, P. O'Leary, and R. Raghavendra, "3D metal printed sierpinski gasket antenna," in *Proc. Int. Conf.Electromagn. Adv. Appl. (ICEAA)*, Sep. 2017, pp. 633–636.
[73] S. Y. Jun, B. Sanz-Izquierdo, E. A. Parker, and J. Franco, "A fractal tetrahedron antenna fabricated using metal 3D printing," presented at the IEEE AP-S Symp. Antennas Propag. USNC-URSI Radio Sci. Meeting, San Diego, CA, USA, 2017.
[74] L. Kumari, "Investigations on stacked aperture coupled fractal microstrip antennas for wireless communication applications," Dept. Electron. Commun. Eng., Thapar Inst. Eng. Technol., Patiala, Punjab, Tech. Rep., Aug. 2018.
[75] K. J. Vinoy, K. A. Jose, V. K. Varadan, and V. V. Varadan, "Resonant frequency of Hilbert curve fractal antennas," in *IEEE Antennas Propag. Soc. Int. Symp. Dig. Held Conjunction USNC/URSI Nat. Radio Sci. Meeting*, vol. 3, Jul. 2001, pp. 648–651.
[76] A. T. M. Sayem and M. Ali, "Characteristics of a microstrip-fed miniature printed Hilbert slot antenna," *Prog. Electromagn. Res.*, vol. 56, pp. 1–18, 2006. [Online]. Available: http://www.jpier.org/PIER/pier.php?paper=0504181. doi: 10.2528/PIER05041801.
[77] R. Kyprianou, B. Yau, A. Alexopoulos, A. Verma, and B. D. Bates, "Investigations into novel multi-band antenna designs," Defence Sci. Technol. Organisation Edinburgh (Australia), Edinburgh, SA, Australia, Tech. note DSTO-TN-0719, 2006.
[78] M. U. Memon, M. M. Tentzeris, and S. Lim, "Inkjet-printed 3D Hilbert-curve fractal antennas for VHF band," *Microw. Opt. Technol. Lett.*, vol. 59, no. 7, pp. 1698–1704, Jul. 2017.
[79] H. Haverkort. (Sep. 2011). "An inventory of three-dimensional Hilbert space-filling curves." [Online]. Available: https://arxiv.org/abs/1109.2323?context=cs
[80] C. Tomko and B. Conner, "Process for strengthening porous 3D printed objects," U. S. 20180079134A1, Mar. 22, 2018.

KERRY JOHNSON is currently pursuing the Ph.D. degree in the material science and engineering program with Youngstown State University, where he is also a Lab Coordinator in the physics program. His current research interests are in 3-D printing and computational modeling of antennas. He is a member of the NSF Program NOA-AGEP.

MICHAEL ZEMBA received the B.Sc. degree in electrical engineering, and the M.Sc. degree in electrical engineering from The University of Akron, Akron, OH, USA, in 2011 and 2013, respectively. He joined the Advanced High-Frequency Branch, NASA's Glenn Research Center, in 2011, and has since worked in the fields of atmospheric propagation and microwave remote sensing, satellite communications, antenna design and metrology, and 3D printing. He has been researching applications of additive manufacturing to antenna design and prototyping, since 2013. He is also the Principal Investigator of the NASA's Atmospheric Propagation Studies Project, which has operated over a dozen tropospheric propagation measurement campaigns for the agency at Ka/Q-band (20 and 40 GHz), V/W-band (70 and 80 GHz), and optical (1550 nm).

BRETT P. CONNER received the B.S. degree in physics from the University of Missouri, in 1998, and the S.M. and Ph.D. degrees in materials science and engineering from the Massachusetts Institute of Technology (MIT), in 2000 and 2002, respectively. He was an Air Force Officer for nine years and his assignments included the Air Force Research Laboratory Materials and Manufacturing Directorate, the Air Force Space Battlelab, Air Force Intern Program – Pentagon, and the Air Force Office of Scientific Research (AFOSR). Subsequently, he was a Defense Contractor for survivability engineering with the Mine Resistant Ambush Protection (MRAP) Joint Vehicle Program Office. He then worked at the Alcoa Technical Center at first in Alcoa Defense managing naval programs and then later in the Alcoa Technology Division developing new alloys and tempers. He joined the faculty of YSU, in 2013. He is currently the Director of the Advanced Manufacturing Research Center, and an Associate Professor of manufacturing engineering with Youngstown State University. His research has been funded by America Makes, the Office of Naval Research, the National Institutes of Standard and Technology (NIST), and the State of Ohio. His research interests include qualification research for aerospace parts produced by metal laser powder bed fusion, linking in-situ monitoring data to the mechanical properties of metal AM parts, the impact behavior of materials fabricated by additive manufacturing, and economic analysis of 3D printing. He has numerous refereed publications and several patents. He is a member of the TMS, SME, ASM, and AFS.

JASON WALKER received the dual-B.S. degree in mechanical engineering and aerospace engineering from Case Western Reserve University, in 2010, and the Ph.D. degree in biomedical engineering from the University of Toledo, in 2014. He completed his postdoc in plastic surgery with the Wexner Medical Center, The Ohio State University. He is currently an Assistant Professor with the Department of Mechanical, Industrial, and Manufacturing Engineering, Youngstown State University. He has over 10 years' experience in additive manufacturing process development, optimization, and materials characterization. He has researched additive manufacturing applications in many different contexts, including metal, polymer, and composite systems for defense, aerospace, smart materials and actuators, and bone tissue engineering.

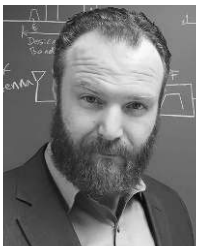

EDWARD BURDEN is currently pursuing the Ph.D. degree in the electrical engineering program with Ohio State University. He is also a term Faculty Member in the electrical and computer engineering program with Youngstown State University. He is the co-author on a conference publication. His current research interests are in 3-D printed antennas and gyrotropic behavior in dielectric materials.

KIRK ROGERS received the Ph.D. degree in materials science and engineering from Purdue University. He completed his postdoctoral work at The Ohio State University. Recently, he was the Technical Leader on the startup of a $40M Additive Manufacturing R&D Center, the culmination of a nearly 20-year career at GE. The majority of his career has been in the medical device manufacturing realm, where he built manufacturing lines for and qualified numerous products. He has 25 years of experience in materials processing, metal additive manufacturing, powder metallurgy, and ceramic matrix composites. He has used additive technologies to solve manufacturing, repair, and supply chain problems for the last 10 years. He has authored and co-authored more than a dozen publications and has been invited to speak on additive and advanced manufacturing topics numerous times. He is a certified Six Sigma Blackbelt.

KEVIN R. CWIOK received the B.S. and M.S. degrees from Embry-Riddle Aeronautical University, Daytona Beach, FL, USA, in 2014 and 2016, respectively. His thesis was on developing passive thermal management systems for plug-in hybrid electric vehicle batteries using phase-change materials with the EcoCAR Team at ERAU. Since graduation, he has become heavily invested within metal additive manufacturing and has over two years of experience within the industry. He was an Engineer at 3D Material Technologies, Daytona Beach, FL, USA, where he learned advanced concepts of part design and parameter development in a range of materials, such as AlSi10Mg and Titanium 6Al-4V. He is currently working with Keselowski Advanced Manufacturing, still within the additive manufacturing industry working to develop new methods of machine parameter and laser control strategies for thermal stress mitigation techniques in higher-stress alloys.

ERIC MACDONALD received the B.S., M.S., and Ph.D. degrees in electrical engineering from The University of Texas at Austin, in 1992, 1997, and 2002, respectively. He worked in industry with IBM and Motorola for 12 years. Subsequently, he co-founded a start-up - Pleiades Technologies, Inc. – developing CAD software and the startup was acquired by Magma Inc. (San Jose, CA, USA), in 2003. From 2003 to 2016, he was with The University of Texas at El Paso as the Associate Director of the W. M. Keck Center for 3D Innovation. He is currently a Professor of electrical and computer engineering and the Friedman Chair for manufacturing with Youngstown State University. He held faculty fellowships at the NASA's Jet Propulsion Laboratory, SPAWAR Navy (San Diego), and a State Department Fulbright Fellowship in South America. His research interests include 3D printed multi-functional applications and process monitoring in additive manufacturing. His recent projects include 3D printing of a nanosatellite with electronics (one of which was launched into Low Earth Orbit in 2013 and a replica of which is on display at the London Museum of Science). He has over 50 refereed publications and patents. He is a member of the ASEE. He is a registered Professional Engineer in Texas.

PEDRO CORTES is currently an Associate Professor with the Department of Civil/Environmental and Chemical Engineering program, as well as in the Materials Science and Engineering Program with Youngstown State University. He has research interests in the area of 3D printing, including smart and multifunctional materials, composite structures, and metal-ceramic systems. He has published several papers in the area of composite structures and 3D printing. His research work has been funded through the Department of Transportation, the Department of Defense, OFRN, NASA, and NSF. He has acted as Faculty Fellow of the Wright-Patterson Air Force Base.